Science of the Total Environment 754 (2021) 142297

Contents lists available at ScienceDirect

Science of the Total Environment

journal homepage: www.elsevier.com/locate/scitotenv

Rapid determination of trace haloacetic acids in water and wastewater using non-suppressed ion chromatography with electrospray ionization-tandem mass spectrometry

Shi Cheng [a], Ya-Ping Wu [a], Tessora R. Young [b], Michael C. Dodd [b], Ji Wu [a], Hao Zhang [c], Zong-Li Huo [c,*], Yu-Ting Qian [d], Yan Li [a], Wen-Tao Li [a,*], Ai-Min Li [a]

[a] State Key Laboratory of Pollution Control and Resources Reuse, School of the Environment, Nanjing University, Nanjing 210023, China
[b] Department of Civil and Environmental Engineering, University of Washington, Seattle, WA, USA
[c] Jiangsu Province Center for Disease Control and Prevention, Nanjing, China
[d] Jiangyin Environmental Monitoring Station, Jiangyin, China

HIGHLIGHTS

- A non-suppressed IC-ESI-MS/MS method was developed for HAA determination.
- Three IC columns including AS16, AS18 and AS24 were compared for HAA separations.
- Different proportions of aqueous methylamine and ACN were tested as mobile phases.
- The optimized method is fast, sensitive, and requires minimal sample workup.
- HAAs were determined in drinking water and wastewater effluents.

GRAPHICAL ABSTRACT

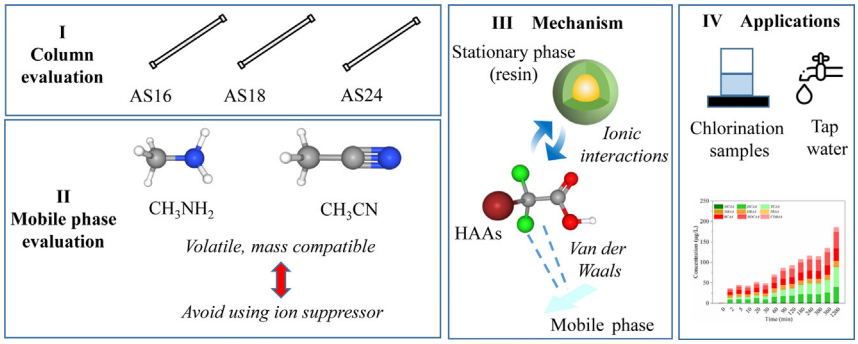

ARTICLE INFO

Article history:
Received 26 June 2020
Received in revised form 23 August 2020
Accepted 7 September 2020
Available online 12 September 2020

Editor: Yolanda Picóa

Keywords:
Haloacetic acids
Disinfection byproducts
IC-ESI-MS/MS
Chlorination
Iodoacetic acids

ABSTRACT

A simple and rapid method employing non-suppressed ion chromatography with electrospray ionization tandem mass spectrometry has been developed for the direct determination of trace-level haloacetic acids (HAAs) in water samples. Using 70/30 (*v*/v) acetonitrile/1 M aqueous methylamine as the mobile phase, three IC columns – AS16, AS18 and AS24 from Thermo-Scientific – were tested, respectively, with the AS16 column exhibiting the best overall performance with respect to resolution and retention time. To assess the effects of mobile phase composition on retention time of HAAs, the AS16 column was further tested using (i) different proportions of acetonitrile to aqueous methylamine, (ii) different proportions of acetonitrile to aqueous solution at fixed methylamine concentrations, and (iii) different concentrations of methylamine at fixed proportions of acetonitrile to aqueous solution. With a low proportion of aqueous solution, van der Waals and/or hydrogen-bonding interactions appeared to play an important role in governing HAA retention, i.e., HAAs with relatively higher apparent logK_{ow}* caused by elevated solvent $^{s}_{s}pK_a$ exhibited longer retention times; whereas with a high proportion of aqueous solution, ionic interactions appeared to dominate retention of HAAs, with the more polarizable HAAs exhibiting longer retention times. Using 70/30 (*v*/v) acetonitrile/1 M aqueous methylamine, the method detection limits were in the range of 0.090–0.216 μg/L for the 11 selected chloro-, bromo- and iodoacetic acids. Finally, this method was applied to monitor HAAs yields in laboratory chlorination experiments and to determine concentrations of HAAs in tap water and wastewater effluent samples.

* Corresponding authors.
E-mail addresses: huozong123@163.com (Z.-L. Huo), liwentao@nju.edu.cn (W.-T. Li).

https://doi.org/10.1016/j.scitotenv.2020.142297
0048-9697/

1. Introduction

Disinfection is a crucial process in water treatment, in which chemical disinfectants such as free chlorine, chloramine, chlorine dioxide or ozone are often utilized to achieve inactivation of pathogenic microorganism. Chlorine-based oxidants are also used to control biofouling and prevention of invasive species introductions (Kinani et al., 2016). Disinfection by-products (DBPs) are inevitably formed in such processes, due to reactions of disinfectants with natural organic matter (NOM) and halide ions in source water (Richardson, 2011; Richardson et al., 2007). To date, over 600 kinds of DBPs have been reported in various forms, and such DBPs in water have drawn considerable public concerns due to their possible long-term health risks for humans, including potential carcinogenicity, mutagenicity and reproductive toxicity (DeMarini, 2020; Richardson et al., 2007; Wagner and Plewa, 2017).

Trihalomethanes (THMs) and haloacetic acids (HAAs) are the most frequently detected DBPs at μg/L levels in chlorinated water (Chen et al., 2008; Krasner et al., 1989; Richardson et al., 2007; Singer et al., 1995; Wang et al., 2020; Xue et al., 2017). There are 9 major HAAs, which include monochloroacetic acid (MCAA), dichloroacetic acid (DCAA), trichloroacetic acid (TCAA), monobromoacetic acid (MBAA), dibromoacetic acid (DBAA), tribromoacetic acid (TBAA), bromochloroacetic acid (BCAA), bromodichloroacetic acid (BDCAA) and chlorodibromoacetic acid (CDBAA) – together comprising the HAA9 group (Zheng et al., 2020). The former 5 HAAs (HAA5) are regulated by the disinfectant/disinfection byproduct rules of the United States Environmental Protection Agency (USEPA), with a maximum contaminant level (MCL) of 60 μg/L for their combined concentration and maximum contaminant level goals (MCLGs) of 70 μg/L for MCAA, zero for DCAA and 20 μg/L for TCAA (USEPA, 2005b). In recent years, some unregulated HAAs have frequently been detected in disinfected water, especially for source waters containing high NOM and bromide or iodide levels (Hu et al., 2018; Krasner et al., 2006). Studies have also shown that bromo- or iodo-DBPs generally have tens to hundreds of times higher toxicity than their chlorinated analogues (Richardson et al., 2008; Richardson et al., 2007; Yang and Zhang, 2013).

The measurement of HAAs in drinking water usually employs derivatization of the carboxylic acid group followed by gas chromatography coupled with electron capture detection (GC-ECD) or mass spectrometry (GC–MS) (Cardador et al., 2008; Sarrión et al., 1999; Urbansky, 2000; Wang et al., 2020; Zhao et al., 2015), and GC–MS/MS is also employed (Kinani et al., 2018). Due to their strong hydrophilicity and acidity, HAAs must be extracted and derivatized into their corresponding methyl esters before GC-based analyses. HAAs can also be separated by ion chromatography (IC) with detection by conductivity (IC-CD) or UV absorbance (IC-UVD) (Barron and Paull, 2004; Liu and Mou, 2003; Liu et al., 2004; Paull and Barron, 2004). However, these IC-CD or IC-UVD methods can be susceptible to interferences from matrix anions and organic constituents present within environmental samples. A 2D-IC system coupling conventional IC and capillary IC with conductivity detection was applied to determine HAA5 (Teh and Li, 2015), for which sub-μg/L (0.38–0.72 μg/L) limits of detection (LODs) were achieved in tap water. Although matrix effects were alleviated in this method, over 60 min of elution time was required for 2D-IC analysis of each sample. Use of IC coupled with inductively coupled plasma-mass spectrometry (ICP-MS) has also been applied for determination of haloacetic acids (Liu et al., 2004; Shi and Adams, 2009), although LODs for chloroacetic acids (MCAA, DCAA and TCAA) were relatively high (15.6–23.6 μg/L as ^{35}ClO).

Notably, electrospray ionization with single or tandem mass spectrometry (ESI-MS/MS) can be coupled with either liquid chromatography (LC) or IC systems (Meng et al., 2010; Wu et al., 2017; Xue et al., 2016). Several studies have reported the trace analyses of HAAs using either reversed-phase columns (C8 and C18) (Li et al., 2012; Luo et al., 2013; Meng et al., 2010) or hydrophilic chromatography columns (HILIC, Phenomenex Luna Amino column) (Dixon et al., 2004). These RPLC or HILIC methods require a complex gradient elution procedure and utilize aqueous organic acid/ion-pair solutions (e.g., formic acid) to achieve an acceptable separation (Dixon et al., 2004; Luo et al., 2013). Using carbonate or hydroxide aqueous solution for elution, IC can easily achieve good separation of HAAs and other ionic compounds. The USEPA Method 557 was established for HAAs analyses using IC-ESI–MS/MS without sample preparation or concentration (USEPA, 2009). Recently, IC with high resolution mass spectrometry has also been used for suspect screening of HAAs in drinking water (Gallidabino et al., 2018). However, this typically necessitates use of specialized IC equipment including an ion suppressor before the mass detector (Roehl et al., 2002; Wu et al., 2017). This can restrict the accessibility of such methods, as ESI-MS/MS systems in typical research and analytical laboratories are more frequently coupled to LC systems without an ion suppressor. The use of an aqueous solution of a volatile base – e.g., methylamine – in place of carbonate or hydroxide eluents can circumvent the need for a suppressor, in turn enabling use of standard LC-ESI-MS/MS systems in a non-suppressed IC-ESI-MS/MS configuration, which has been applied in USEPA Method 331.0 for perchlorate (USEPA, 2005a). In addition, the USEPA Method 557 requires almost one hour for each analysis (USEPA, 2009), which is still time-consuming. Recently, it has been reported that adding acetonitrile into hydroxide eluents could significantly shorten the total run time for IC-ESI-MS/MS analyses of HAAs (Wu et al., 2017).

In this study, we sought to develop a rapid, sensitive and selective IC-ESI-MS/MS method for the analyses of chloro-, bromo- and iodoacetic acids based on a conventional LC-ESI-MS/MS system without ion suppression. Three IC columns were evaluated with mobile phases comprising various proportions of acetonitrile and aqueous methylamine. Chromatographic conditions were optimized and the effects of chromatographic conditions on retention/elution of HAAs were examined with respect to their apparent $\log K_{ow}$* values and polarizabilities. Finally, the optimized non-suppressed IC-ESI-MS/MS method was applied to monitor HAA formation during laboratory chlorination experiments and to detect occurrence and concentrations of HAAs in tap water and wastewater effluent samples.

2. Materials and methods

2.1. Chemical standards and reagents

MBAA (≥99%), DBAA (>98%), BCAA (97%), TCAA (≥99%), TBAA (99%), BDCAA (99%), CDBAA (97%), monoiodoacetic acid (MIAA, ≥98.0%) and the internal standard MBAA-$2C^{13}$ (≥99%) were purchased from Sigma-Aldrich Ltd. MCAA (99%) and DCAA (99%) were ordered from Tokyo Chemical Industry Co. Ltd. Diiodoacetic acid (DIAA) was purchased from Toronto Research Chemicals without information about its purity. Working solutions of each HAA were prepared in water at 100 μg/L for optimizing mass detector parameters. A mixed standard solution of HAA9 in methyl *tert*-butyl ether (2000 μg/mL, Sigma-Aldrich) was used for preparing standard curves, together with separate MIAA and DIAA standards. Working solutions of HAAs were prepared daily at lower concentrations by serial dilution in pure water.

A natural organic matter (NOM) isolate was purchased from the International Humic Substances Society (Catalog No. 2R101N, Suwannee River NOM, designated as SR_NOM hereafter). An NaOCl solution containing 4.00–4.99% free available chorine (FAC) in *w*/*v* was purchased from Sigma-Aldrich, and its FAC concentration was spectrophotometrically standardized at $\lambda = 292$ nm ($\varepsilon_{292nm,\ OCl^-} = 350\ M^{-1}\ cm^{-1}$) before use in chlorination experiments (Kumar et al., 1986).

Aqueous methylamine solution (40 wt%, Sigma-Aldrich) and acetonitrile (ACN, HPLC grade, Merck) were used to prepare mobile phases. Note that the preparation of aqueous methylamine solution should be operated in fume hood to avoid inhalation of methylamine.

2.2. IC-ESI-MS/MS analysis

IC-ESI-MS/MS analyses were performed using an Agilent 1290 LC system coupled with an AB Sciex Qtrap 5500 MS/MS, with no ion suppressor installed between the LC and MS systems. For separations, three Dionex™ IonPac™ IC columns – AS16, AS18 and AS24 (microbore separator, 2 mm × 250 mm) – were assessed for their compatibility and utility with the mobile phase of 1 M aqueous methylamine solution (typically 30%, Solvent A) and ACN (typically 70%, Solvent B). An HPLC injection volume of 10 μL was used for sample analyses. To be compatible with the column inner diameter, the flow rate was 300 μL/min. The column temperature was 30 °C. Various chromatographic conditions were evaluated for the selected AS16 IC column, including type of organic solvent (methanol vs acetonitrile as Solvent B), concentration of aqueous methylamine (0.5 M vs 1 M as Solvent A), and proportion of aqueous methylamine solution vs acetonitrile: 20/80, 30/70, 35/65 and 40/60 for 0.5 M aqueous methylamine solution (Solvent A) vs acetonitrile (Solvent B), and 10/90, 15/85, 20/80, 25/85, 30/70, and 35/65 for 1 M aqueous methylamine solution (Solvent A) vs acetonitrile (Solvent B). The methylamine concentration in mobile phase can be calculated by multiplying the concentration of aqueous methylamine (0.5 M or 1 M in Solvent A) by its applied proportion. To avoid evaporation and inhalation of organic solvents and methylamine, stay-safe caps were installed on the solvent bottle and waste eluent tank.

The Turbo V ion source of the Qtrap 5500 MS/MS was operated using an electrospray needle in negative mode. Ionization source parameters were as follows: curtain gas pressure = 30.0 psi; collision gas = medium; ion spray voltage = −4500.0 V; temperature = 450.0 °C; ion source gas 1 pressure = 40.0 psi; ion source gas 2 pressure = 40.0 psi.

For MS/MS analyses, multiple reaction monitoring (MRM) mode of the Qtrap 5500 MS/MS was used for qualitative and quantitative analyses. The corresponding physicochemical properties and MS/MS parameters for each analyte – obtained by flow injection analyses – are listed in Table 1. Most HAAs were analyzed using two transitions.

2.3. Data acquisition and method evaluation

Data acquisition and analysis were undertaken using AB Sciex Analyst and MultiQuant software. Eight-point calibration curves were established for each standard HAA at concentrations of 0.5, 1, 5, 10, 20, 50, 100 and 200 μg/L, respectively. Each calibration standard was spiked with 5 μg/L MBAA-$2C^{13}$ as internal standard and measured in duplicate.

For assessing method stability and precision, the intra-day and inter-day precision tests were conducted for all analytes across a three-day period (Wu et al., 2017). For the first day as intra-day test, the fortified samples spiked with 5 μg/L of analytes were analyzed in triplicate every 4 h for 3 times within a day ($n = 9$). For the second and third day, fortified samples were analyzed in triplicate on each day. Seven fortified replicate samples were prepared by spiking analytes at a concentration of 2–5 times the estimated noise level in ultrapure water. The spiked concentration was 0.5 μg/L for each HAA. The method detection limits (MDLs) were calculated as the products of the standard deviations of measured concentrations and the Student's t value for the 99% confidence level with 6 degrees of freedom (for seven replicate determinations, the t-value is 3.143).

Recoveries of the 11 analytes were determined using a tap water sample from Nanjing. Referring to literature (Wu et al., 2017), the fortified triplicate samples were prepared by spiking 10 μg/L of all analytes, 10 μg/L of internal standards and 100 mg/L of NH_4Cl into the tap water sample. NH_4Cl was added to remove residual chlorine in tap water (USEPA, 2009).

Although MRM mode can provide primary confirmation of analyte identity by enabling exclusive analyses of a targeted compound, secondary confirmation of the identity of HAAs in chlorinated NOM solutions and tap water was also undertaken by comparing retention times with corresponding standards. Each sample was spiked with 5 μg/L MBAA-$2C^{13}$ as internal standard.

Table 1
Physicochemical properties and mass parameters of HAAs.

Analytes	Physicochemical properties[a]					Q1[b]		Q3[b]		CE (eV)	CXP (V)	DP (V)	EP (V)
	pK_a	$^{s}_{s}$pK_a (10/90)[c]	logK_{ow}	logK_{ow}* (10/90)[c]	Polarizability (Å^3)	*m/z*	Transition	m/z	Transition				
MCAA	2.87	9.1	0.22	−3.20	(7.00)	92.8	$[M-H]^-$	34.9	$[^{35}Cl]^-$	−19	−12	−20	−11
DCAA	1.26	6.53	0.92	−5.07	(8.98)	126.8	$[M-H]^-$	82.9	$[M-COOH]^-$	−13	−11	−20	−12
						126.8	$[M-H]^-$	34.8	$[^{35}Cl]^-$	−22	−11	−20	−12
TCAA	0.51	5.33	1.33	−5.86	(10.98)	116.8	$[M-COOH]^-$	34.8	$[^{35}Cl]^-$	−19	−16	−20	−10
						160.8	$[M-H]^-$	116.8	$[M-COOH]^-$	−11	−16	−20	−10
MBAA	2.89	9.14	0.41	−2.97	(8.17)	138.8	$[M-H]^-$	80.9	$[^{81}Br]^-$	−15	−9	−20	−13
						136.8	$[M-H]^-$	78.8	$[^{79}Br]^-$	−15	−9	−20	−13
DBAA	1.48	6.89	(0.7)	−4.93	(11.41)	216.6	$[M-H]^-$	172.7	$[M-COOH]^-$	−14	−11	−20	−11
						216.6	$[M-H]^-$	78.8	$[^{79}Br]^-$	−19	−11	−20	−11
TBAA	0.72	5.67	(1.71)	−5.14	(14.68)	250.7	$[M-H]^-$	78.7	$[^{79}Br]^-$	−19	−13	−20	−12
						252.7	$[M-H]^-$	80.8	$[^{81}Br]^-$	−19	−13	−20	−12
BCAA	(1.97)	(7.67)	(0.61)	−4.24	(10.17)	172.8	$[M-H]^-$	128.7	$[M-COOH]^-$	−13	−14	−20	−13
						172.8	$[M-H]^-$	80.9	$[^{81}Br]^-$	−17	−14	−20	−13
BDCAA	(1.45)	(6.84)	(1.53)	−4.15	(12.18)	162.8	$[M-COOH]^-$	78.8	$[^{79}Br]^-$	−20	−6	−20	−6
						164.8	$[M-COOH]^-$	80.8	$[^{81}Br]^-$	−20	−6	−20	−6
CDBAA	(1.12)	(6.31)	(1.62)	−4.59	(13.41)	206.7	$[M-COOH]^-$	78.8	$[^{79}Br]^-$	−7	−14	−20	−6
						208.7	$[M-COOH]^-$	80.8	$[^{81}Br]^-$	−7	−14	−20	−6
MIAA	3.18	(9.61)	(0.85)	−2.06	(10.51)	184.9	$[M-H]^-$	126.8	$[^{127}I]^-$	−17	−13	−30	−10
DIAA	(2.29)	(8.18)	(1.53)	−2.81	(16.08)	266.7	$[M-COOH]^-$	127.0	$[^{127}I]^-$	−30	−10	−40	−12
						310.8	$[M-H]^-$	266.7	$[M-COOH]^-$	−7	−10	−40	−12
MBAA-$2C^{13}$	–	–	–		–	140.8	$[M-H]^-$	80.9	$[^{81}Br]^-$	−23	−10	−20	−13

[a] pK_a and logK_{ow} values were obtained from the PubChem database (https://pubchem.ncbi.nlm.nih.gov/), polarizability values were obtained from the Chemicalize website (https://chemicalize.com/), where the values in the parentheses are estimated data; $^{s}_{s}$pK_a and logK_{ow}* values were calculated as described below and in text S1, and in Tables S3-S6. Note that logKow values are for the undissociated (neutral) forms of the HAAs, whereas logK_{ow}* values are "apparent" values for the combination of the undissociated and dissociated (anionic) species under the designated mobile phase conditions.

[b] The Q1/Q3 pair in the first row is for quantitative analysis and the Q1/Q3 pair in the second row is for qualitative analysis.

[c] The (10/90) represents the proportion of 1 M aqueous methylamine vs ACN.

2.4. Chlorination experiments

For laboratory chlorination experiments, a 100 mL SR_NOM solution containing 2 mg/L dissolved organic carbon (DOC), 50 mg/L Cl^-, and 200 μg/L Br^- was prepared in a 100 mL amber glass bottle. The NOM solution was then spiked with 4 mg/L Cl_2 and kept at room temperature (25 °C). Samples were collected with a 1 mL pipette at specific chlorination times as follows: 0, 2, 5, 10, 20, 30, 60, 90, 120, 180, 240, 300, 360 and 1200 min. Residual chlorine was quenched by the addition of 20 mM Na_2SO_3 in a molar ratio of Na_2SO_3/HOCl = 1.2.

2.5. Environmental applications

Tap water samples were collected from laboratories in Nanjing University and Jiangyin Environmental Monitoring Station by the addition of 100 mg/L NH_4Cl for quenching residual chlorine, both of which utilize the Yangtze River as a drinking water source. A wastewater effluent sample (DOC 13.2 mg/L) was collected from a textile wastewater treatment plant, where ~50 mg/L Cl_2 was added for decoloration and the residual chlorine was naturally decayed. Samples were filtered through 0.22 μm syringe filters and the wastewater sample was further diluted 50 times with pure water prior to IC-ESI-MS/MS analysis.

3. Results and discussion

3.1. Selection of IC columns

Reported IC-MS/MS methods for determination of HAAs and other environmental contaminants typically employ hydroxide eluent for anion exchange, necessitating the use of an ion suppressor prior to the mass spectrometer (Wu et al., 2017). Based on specifications obtained from datasheets of the Dionex™ IonPac™ AS16, AS18 and AS24 columns (Table S1), the polymer skeletons and functional groups of these columns are 55% crosslinked divinylbenzene and alkanol quaternary ammonium ion, which can be operated over a pH range of 0–14 and with 0–100% HPLC-compatible organic solvents. By using methylamine – a weak and volatile organic base (pK_a = 10.6) (Espinosa et al., 2002) – in place of sodium or potassium hydroxide, it is possible to prepare MS-compatible aqueous solutions with a sufficiently high pH to enable IC column elution, while enabling operation of standard LC-ESI-MS/MS instrumentation without a suppressor, in a non-suppressed IC-ESI-MS/MS mode (USEPA, 2005a). For example, the pH of a 0.2 M aqueous methylamine solution is calculated as 11.96, consistent with pH ~ 12 in US EPA Method 331.0 (USEPA, 2005a). Furthermore, addition of ACN to mobile phases has been found to yield shorter elution times and improved chromatography for HAAs and other organic acid analytes (Gilchrist et al., 2015; Wu et al., 2017).

Thus, the three candidate anion exchange columns (i.e., AS16, AS18, and AS24) were evaluated on the LC-ESI-MS/MS system with a test mobile phase of 70/30 (*v*/v) acetonitrile/1 M aqueous methylamine solution, i.e., 0.3 M methylamine in the mixed mobile phase. Fig. 1a–c illustrate the individual chromatograms of the 9 HAAs separated by each of these three IC columns. With the AS16 column, the 9 HAAs were eluted rapidly (within 3.99–5.23 min). The rapid elution of HAAs from the AS16 column can be attributed to its low column capacity (Table S1). The AS18 and AS24 columns showed good separation of HAAs, but long retention times. Additionally, use of both of the latter columns resulted in much lower sensitivities and a higher noise level in comparison with the AS16 column.

With respect to the HAAs' elution sequence (Fig. 1 and Table S2), the AS16 and AS24 columns showed similar orders, with TCAA < DCAA < MCAA, MBAA < DBAA < TBAA, and BDCAA < DBCAA, which generally follows the order of decreasing number of Cl atoms and increasing number of Br atoms. The retention time ratios of each HAA for the AS24 relative to those for the AS16 remained in the range of 4.27–4.47. These results suggest that the properties of the packing materials in the AS24 and AS16 are quite similar. The differences in retention time can be attributed mainly to differences in column capacity (140 μeq vs 42.5 μeq) and particle size (7 μm vs 9 μm), as listed in Table S1. The high column capacity and small particle size of the AS24 column resulted in more effective separation but longer retention time than the AS16 column.

With the AS18 column, the HAAs were eluted in the order of increasing number and decreasing electronegativity (Cl > Br) of halogen atoms, i.e., MCAA < MBAA < DCAA < BCAA < DBAA < TCAA < BDCAA < CDBAA < TBAA. The good linear correlations between retention time and HAA polarizability (Fig. S1, R^2 = 0.964) suggest that ionic interactions of the HAAs with the stationary phase principally affected their retention by the AS18 column, with elution mediated by OH^- from ionization of methylamine. In prior studies, the highly polarizable HAAs such as TCAA, BDCAA, CDBAA, and TBAA were usually the last species in ion chromatography to be eluted by aqueous hydroxide solutions (Gilchrist et al., 2015; Liu et al., 2004; Shi and Adams, 2009; Wu et al., 2017).

On account of its ability to yield adequate HAA separation over shorter elution times compared to the AS18 or AS24 columns, the AS16 column was selected for further development of the non-suppressed IC-ESI-MS/MS method for HAA analyses.

3.2. Evaluation and selection of chromatographic conditions

For ion chromatography, the ionic, hydrophobic, and/or hydrogen-bonding interactions among analytes, stationary phase, and mobile phase, as well as the physicochemical properties of analytes, determine overall retention time. Hence, chromatographic conditions were next evaluated by varying methylamine concentrations and/or proportions of aqueous solution vs ACN. As shown in Figs. 2, S2, S3 and Table 2, increasing the respective proportions of aqueous 0.5 M or 1 M methylamine solutions (Solvent A) from 20% to 40% or from 10% to 35% significantly decreased the elution times of the HAAs and the total method run time. Interestingly, the elution sequences of HAAs also reversed with increasing proportions of aqueous methylamine solution. For chloroacetic acids, the sequence changed gradually from TCAA < DCAA < MCAA to MCAA < DCAA < TCAA when the proportion of 0.5 M aqueous methylamine solution (Solvent A) reached 40%. For bromoacetic acids, the sequence changed from TBAA < DBAA < MBAA to MBAA < DBAA < TBAA when the proportion of aqueous 1 M methylamine solution (Solvent A) reached 30%. These phenomena suggest that the principal interactions among stationary phase, mobile phase, and analytes change along with changes in mobile phase composition.

For chloro- and bromoacetic acids, the magnitudes of pK_a values decrease with increasing number of Cl or Br; whereas $\log K_{ow}$ values of the HAAs generally increase with increasing Cl or Br number (Table 1). As shown in Table S4, at high proportions of ACN, the "apparent" pK_a values of HAAs in ACN-water solvent (${}^{s}_{s}pK_a$) increase significantly from the pK_a values of the same compounds in water (${}^{w}_{w}pK_a$), because ACN is a poor hydrogen bond donor, with weak solvation of H^+ relative to water (Espinosa et al., 2002; Rossini et al., 2018). The $\log K_{ow}$ values in Table 1 correspond to the undissociated forms of each HAA. Because the proportion of the HAAs present in their undissociated form, α, increases with increasing ACN proportion for a given pH (Table S5), the "apparent" $\log K_{ow}{}^*$ values of each HAA likewise increase with increasing proportion of ACN (Table S6). The details for ${}^{s}_{s}pK_a$ and $\log K_{ow}{}^*$ calculation are described in Text S1.

At low proportions (e.g., 10%–15%) of 1 M aqueous methylamine solution (i.e., 0.1 M or 0.15 M methylamine in mobile phase), the apparent $\log K_{ow}{}^*$ values for chloro- or bromoacetic acids decrease with increasing Cl or Br number (Tables 1 and S6), which is mainly attributed to their dependence on analyte ${}^{s}_{s}pK_a$ and mobile phase pH. Under these conditions, the apparent $\log K_{ow}{}^*$ values and retention times – especially those of the chloroacetic acids – showed strong positive correlations (Fig. S4, R^2 > 0.9). This may in part reflect a role of enhanced

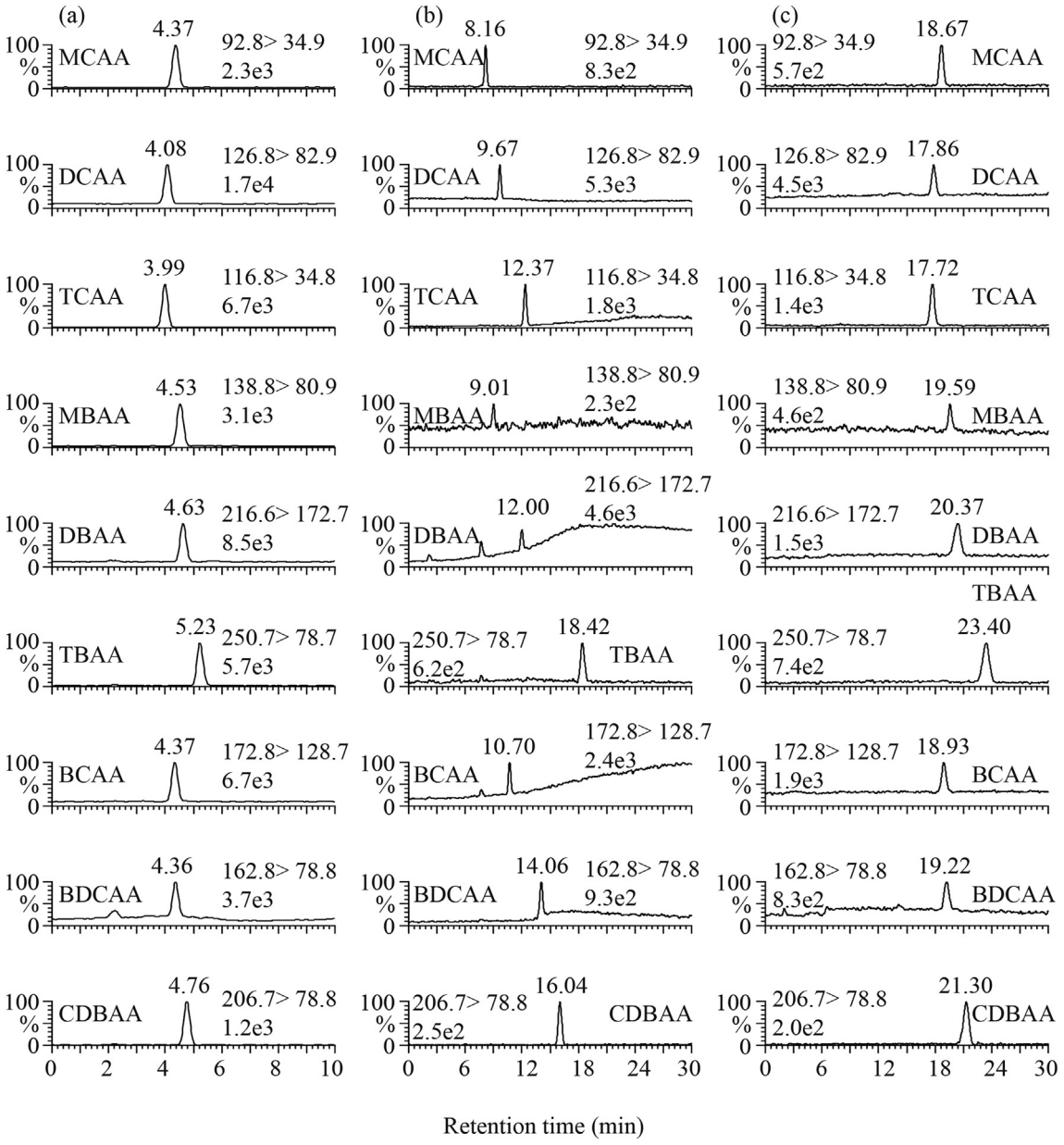

Fig. 1. The non-suppressed IC-ESI-MS/MS chromatograms of nine HAA standards (10 μg/L) with different anion exchange columns: (a) AS16, (b) AS18, and (c) AS24. The mobile phase comprised 0.3 M methylamine in 30% water and 70% ACN. The number on top of each chromatogram peak is the retention time.

hydrophobic (van der Waals non-specific) interactions of the neutral forms of the HAAs with the AS16 phase under such conditions. An additional explanation could derive from an elevated role of hydrogen bonding between (1) the more highly protonated H-donating/accepting -COOH groups of the less halogenated (and weaker acid) HAAs and (2) the octanol-like H-accepting/donating -ROH groups of the alkanol side-chains of the AS16 alkanol quaternary ammonium stationary phase under such conditions (noting that the anionic forms of the HAAs' carboxylate groups can only H-accept, and not H-donate). That is, the strong correlations between the HAAs' logK_{ow}* values and retention times may reflect an overall favorability of neutral HAA species partitioning from weakly protic, high-ACN/low-H_2O mobile phase to the alkanol-enriched stationary phase, due to enhancement of both non-specific van der Waals and specific hydrogen bonding interactions with the latter relative to the former. Previous observations that high proportions of aprotic/weakly-H-accepting ACN lead to greater increases in retention of various organic acids on an AS18 alkanol quaternary ammonium stationary phase compared to similar proportions of protic/strongly-H-accepting MeOH are also consistent with a role of enhanced H-bonding between analytes and the stationary phase in the presence of ACN (Gilchrist et al., 2015).

For mobile phases containing the same methylamine concentration but different proportions of aqueous vs ACN (e.g., 1 M aqueous methylamine as Solvent A at 10% proportion vs 0.5 M aqueous methylamine as Solvent A at 20% proportion in Table 2), higher proportions of aqueous phase significantly lowered HAA retention times, consistent with the resulting decreases in their apparent logK_{ow}*, $^{s}pK_a$ and α values and consequent weakening of their van der Waals and hydrogen bonding interactions with the AS16 phase under such conditions (as the proportion of protonated HAAs decreases and the mobile phase composition becomes more aqueous/protic). In addition, as shown in Table 2, mobile phases with matched proportions of aqueous/ACN but different methylamine concentrations (e.g., 0.1 M or 0.2 M methylamine in mobile phase comprising 20% aqueous proportion) showed similar retention times

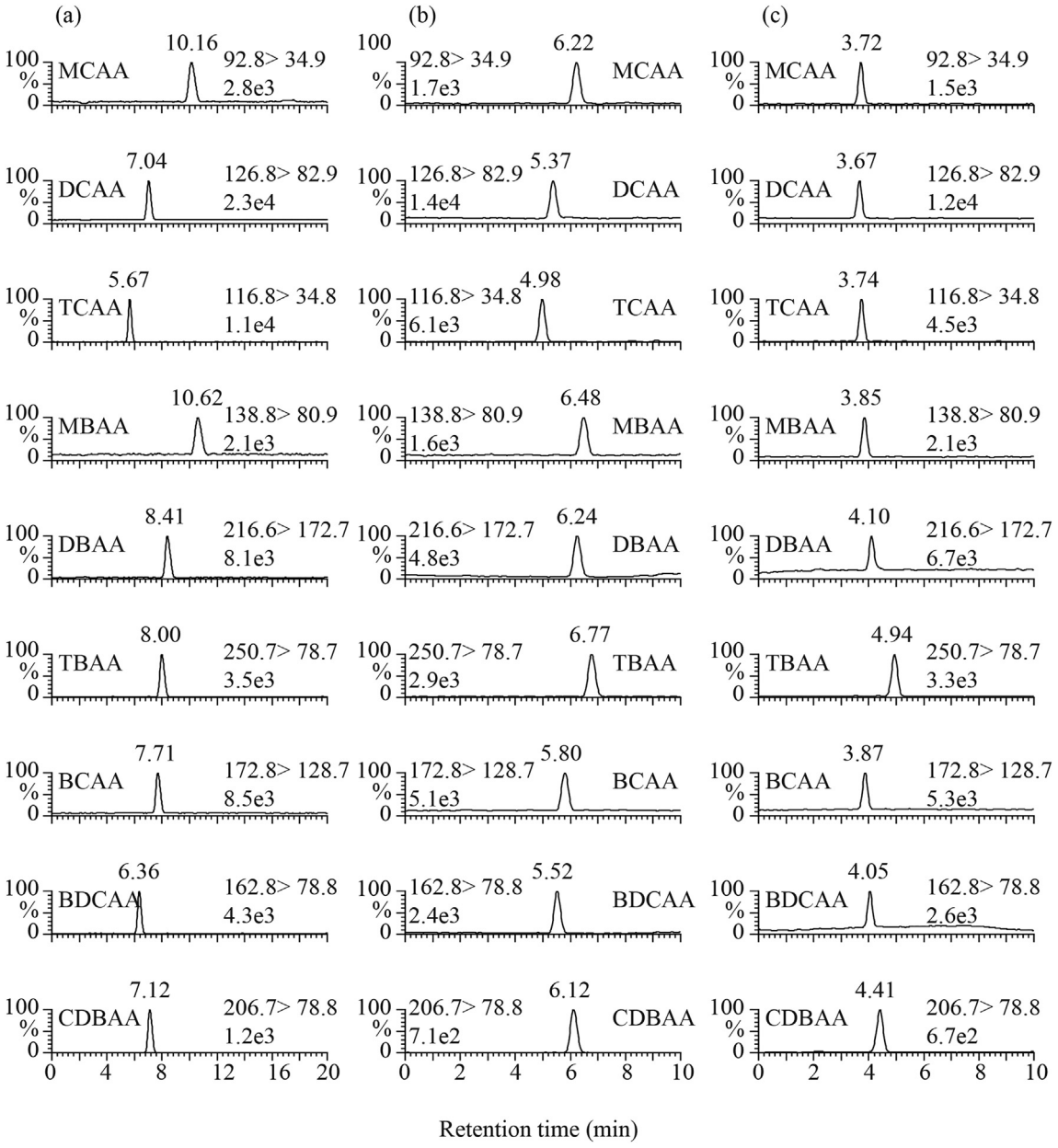

Fig. 2. Non-suppressed IC-ESI-MS/MS chromatograms of nine HAA standards (10 μg/L) at (a) 15%, (b) 25%, and (c) 35% of 1 M aqueous methylamine solution, with ACN comprising the remaining % of the mobile phase. The number on top of each chromatogram peak is the retention time.

Table 2
Retention times (min) of each HAA on the AS16 column for varying proportions of aqueous methylamine solution as Solvent A and ACN as Solvent B comprising the remaining %, corresponding to the data shown in Figs. 2, S2, and S3.

HAAs	Proportions of 1 M aqueous methylamine as Solvent A						Proportions of 0.5 M aqueous methylamine as Solvent A			
	10%	15%	20%	25%	30%	35%	20%	30%	35%	40%
MCAA	22.28	10.16	9.65	6.22	4.37	3.72	9.18	5.22	4.43	4.01
DCAA	12.69	7.04	7.25	5.37	4.08	3.67	7.05	4.86	4.38	4.14
TCAA	9.04	5.67	6.16	4.98	3.99	3.74	6.07	4.78	4.50	4.37
MBAA	23.63	10.62	10.16	6.48	4.53	3.85	9.61	5.44	4.62	4.17
DBAA	15.86	8.41	8.78	6.24	4.63	4.10	8.41	5.63	5.00	4.77
TBAA	13.57	8.00	9.03	6.77	5.23	4.94	8.68	6.51	6.22	6.22
BCAA	14.26	7.71	7.99	5.80	4.37	3.87	7.71	5.22	4.67	4.34
BDCAA	10.36	6.36	6.98	5.52	4.36	4.05	6.82	5.29	4.95	4.96
CDBAA	11.86	7.12	7.92	6.12	4.76	4.41	7.69	5.86	5.34	5.53

for each HAA, further suggesting that ionic interactions were apparently superseded by the influence of van der Waals and/or hydrogen bonding interactions between HAAs and the stationary phase under conditions of low aqueous phase and high ACN proportion.

In contrast, at higher proportions of aqueous methylamine as Solvent A (>30%), retention times of the HAAs – especially those of Br-containing HAAs – exhibited positive correlations with their polarizabilities (Fig. S5). When increasing the proportion of 1 M aqueous methylamine as Solvent A from 20% to 30%, van der Waals and/or hydrogen-bonding interactions of the HAAs with the AS16 phase appeared to become weaker along with the decrease of apparent logK_{ow}*, and the strength of ionic interactions (proportional to HAA polarizabilities) appeared to become predominant in governing retention of the HAAs. At higher proportions of aqueous solution (e.g., 30–35%), an increase of aqueous methylamine concentration from 0.5 M to 1 M in Solvent A also shortened HAA retention times (Table 2), consistent with a

dominant role of ionic interactions in governing HAA elution. At a 40% proportion of 0.5 M aqueous methylamine (Solvent A), the elution order of chloroacetic acids fully reversed (from TCAA < DCAA < MCAA to MCAA < DCAA < TCAA), suggesting that under these conditions van der Waals and/or hydrogen-bonding interactions between chloroacetic acids and stationary phase (which are positively correlated with the HAAs' "apparent" logK_{ow}* values; Table S6) gave way to ionic interactions (which are positively correlated with HAA polarizabilities; Table 1).

Variations in relative signal intensity of each HAA versus the proportion of aqueous methylamine solution used are plotted in Fig. S6. For a mobile phase with 0.5 M aqueous methylamine (Solvent A), increasing the proportion of the aqueous methylamine solution resulted in divergent trends in relative peak intensities of HAAs (i.e., increased signal intensities for DBAA and BDCAA, and decreasing signal intensities for the others). However, the chromatograms of DBAA and BDCAA also exhibited high baseline intensities, leading to lower sensitivities. For a mobile phase with a 1 M aqueous methylamine solution as Solvent A, chromatograms generally exhibited sharper HAA peak shapes than for 0.5 M aqueous methylamine as Solvent A (Figs. 2 and S3). A mobile phase containing 0.3 M methylamine (i.e., 1 M aqueous methylamine mixed with ACN in 30/70 *v*/v) exhibited the highest peak intensity for MBAA, DBAA and TBAA. The chromatographic resolution values of HAAs under different proportion of aqueous methylamine solution are calculated and summarized in Table S7, suggesting that higher separation can be achieved by using low concentrations of methylamine or low proportions of aqueous methylamine or gradient elution (Fig. S8). The mobile phase with 30% proportion of Solvent A using 1 M aqueous methylamine solution (i.e., 0.3 M methylamine in mobile phase) was selected for method validation and quantification, in light of its short analysis time and higher tolerance to levels of inorganic salts likely to be encountered in environmental samples. Although the chromatographic resolution values were relatively low, the adjacent HAAs can be further distinguished by their unique precursor ions and product ions in ESI-MS/MS MRM mode.

3.3. Linearity, limits of detection, recovery and precision

Calibration curves were established from concentrations of 0.5 μg/L to 200 μg/L for each HAA, and exhibited good linearity with correlation coefficients (r) > 0.995 (Table 3). A 5.0 μg/L concentration of internal standard MBAA-2C^{13} was spiked into the calibration standards and environmental samples, and all HAAs in samples were internally calibrated using relative response factors (Wu et al., 2017). The MDLs of HAAs were found to be in the range of 0.090–0.216 μg/L, i.e., sub-μg/L in all cases. Notably, MDLs of 0.090 μg/L and 0.208 μg/L were also determined for MIAA and DIAA, respectively, demonstrating that the non-suppressed IC-ESI-MS/MS method is sensitive and useful for measurement of iodoacetic acids in addition to the chloro- and bromoacetic acids comprising HAA9. As shown in Table 3, the mean recoveries for all analytes were 83.9–110.0% with RSDs less than 8.4 in the Nanjing tap water, comparable to the recovery of 80.0–103.0% in chlorinated surface water in EPA Method 557 (USEPA, 2009). Intra-day RSDs (n = 9) of peak area ranged from 3.3% to 7.1%, with a median of 5.4%, and inter-day RSDs (n = 9) of peak area ranged from 3.4% to 10.4% with a median of 7.0%. The inter-day RSDs of retention time were less than 1.5%. Note that to prevent drift of retention times, a stay-safe cap should be installed onto the mobile phase bottles to avoid evaporation of methylamine and ACN.

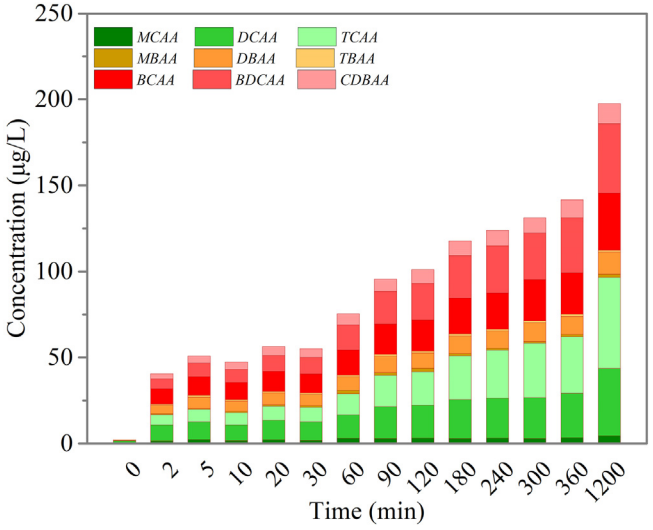

Fig. 3. HAA9 formation versus time during chlorination of SR_NOM solution (at 4 mg/L as Cl_2, 200 μg/L Br^-, and 2.0 mg/L DOC).

In general, these results show that the non-suppressed IC-ESI-MS/MS method enables highly sensitive and precise HAA analyses and provides an alternative to reported suppressed IC-ESI-MS/MS methods and EPA Method 557 (USEPA, 2009; Wu et al., 2017), with decreased method run-time and system complexity (Table S9).

3.4. Environmental application

The optimized non-suppressed IC-ESI-MS/MS method was applied to monitor HAA9 formation during chlorination of a solution of SR_NOM (at 4 mg/L as Cl_2, 200 μg/L Br^-, and 2.0 mg/L DOC). Since the solution was prepared without iodide, the iodoacetic acids were not monitored. As shown in Fig. 3 & Table S8, HAAs rapidly formed (up to 42.54 μg/L total concentration) over the first 2 min of reaction, and the concentrations of most HAA species generally continued to increase with increasing reaction time. The predominant HAA species observed were DCAA, TCAA, BCAA, and BDCAA, which represented 72.5–84.0% of total HAA mass concentrations.

Table 3
Calibration curve linearity, detection limits, mean recoveries and RSDs for all HAAs.

Analyte	Regression equation	r value	MDL (μg/L)	Recovery (%) ± RSD (%)	Intra-day RSD (%) (n = 9)		Inter-day RSD (%) (n = 9)	
					Retention time	Area	Retention time	Area
MCAA	y = 3088.69277 x + 282.80056	0.9984	0.140	98.0 ± 5.7	1.5	3.3	1.2	10.4
DCAA	y = 17,586.27106 x + 1811.62788	0.9976	0.157	90.4 ± 3.4	1.3	6.9	1.2	7.0
TCAA	y = 8166.58858 x + 282.92132	0.9979	0.216	94.7 ± 1.8	1.3	6.7	1.1	5.8
MBAA	y = 4085.45791 x + 346.26579	0.9991	0.146	98.1 ± 8.3	1.5	7.1	1.3	4.5
DBAA	y = 10,823.77858 x + 147.10970	0.9990	0.129	103.7 ± 8.4	1.5	4.1	1.2	7.4
TBAA	y = 8425.60547 x + 170.62205	0.9993	0.093	83.9 ± 4.8	1.5	5.4	1.2	6.0
BCAA	y = 8465.33678 x + 458.46833	0.9984	0.196	110.0 ± 2.0	1.4	4.8	1.1	5.8
BDCAA	y = 4141.01009 x + 344.75120	0.9983	0.187	100.1 ± 1.0	1.4	5.4	1.1	7.7
CDBAA	y = 1791.96941 x + 82.39549	0.9991	0.107	90.0 ± 5.4	1.4	4.5	1.2	7.5
MIAA	y = 3176.29987 x + 44.32015	0.9994	0.090	94.0 ± 3.6	1.5	5.6	1.2	3.4
DIAA	y = 26,171.18476 x – 202.46509	0.9991	0.208	93.8 ± 6.1	1.4	3.7	1.4	8.5

Table 4
The occurrence and concentrations of HAAs in tap water and wastewater effluent in Nanjing and Jiangyin, China.

	Nanjing tap water (n = 3)	Jiangyin tap water (n = 3)	Textile Wastewater (n = 2)
	Conc. (μg/L) ± RSD (%)	Conc. (μg/L) ± RSD (%)	Conc. (μg/L) ± SD (μg/L)
MCAA	0.20 ± 8.0%	0.10 ± 3.9%	44.50 ± 0.75
DCAA	1.85 ± 6.6%	2.03 ± 5.3%	648.33 ± 32.52
TCAA	2.23 ± 3.2%	8.03 ± 1.9%	1113.30 ± 27.55
MBAA	N.D.	N.D.	N.D.
DBAA	0.65 ± 5.4%	0.42 ± 2.5%	2.35 ± 0.05
TBAA	0.95 ± 2.3%	1.49 ± 2.1%	N.D.
BCAA	0.54 ± 5.3%	0.44 ± 6.5%	34.58 ± 0.93
BDCAA	1.26 ± 4.4%	1.70 ± 13.0%	100.68 ± 0.73
CDBAA	0.79 ± 10.5%	0.70 ± 5.9%	8.88 ± 0.93
MIAA	N.D.	N.D.	N.A.
DIAA	N.D.	N.D.	N.A.
HAA9	8.47	14.91	1952.62

Note: N.D., not detected; N.A., not available, because the textile wastewater sample was analyzed before the MS/MS parameters for MIAA and DIAA were optimized.

The optimized non-suppressed IC-ESI-MS/MS method was also applied to monitor the occurrence and concentrations of HAAs in tap water and chlorinated textile wastewater effluent (Table 4). In an application example of USEPA Method 557 (USEPA, 2009), the RSDs of HAA9 were between 1.4% and 11%. The RSDs of this non-suppressed IC-ESI-MS/MS method were generally less than 10% in measurements of HAAs in tap water, indicating that this method has comparable repeatability to the USEPA Method 557.

The total concentrations of HAA9 measured in Nanjing and Jiangyin tap waters were 8.47 μg/L and 14.91 μg/L, respectively. TCAA, DCAA, BDCAA and TBAA were the predominant species detected – contributing up to 74.4% (Nanjing) and 88.9% (Jiangyin) of HAA mass concentrations. MBAA was not detected in either tap water sample. For iodoacetic acids, neither MIAA nor DIAA were detected in Nanjing or Jiangyin tap waters. For the chlorinated textile wastewater effluent, the measured total HAA9 level was extremely high (1952.62 μg/L), with TCAA (~57.0% by mass) and DCAA (~33.2% by mass) as the predominant species.

4. Conclusion

A rapid and sensitive non-suppressed IC-ESI-MS/MS method has been developed for the determination of trace-level haloacetic acids (HAAs) in environmental water samples, which requires no sample extraction, derivatization, or other preparatory sample workup. Using a mixture of acetonitrile and aqueous methylamine as the mobile phase, the retention times and elution sequences of HAAs appear to be governed to varying degrees by ionic, van der Waals, and/or hydrogen-bonding interactions among stationary phase, mobile phase, and analytes, depending on mobile phase composition.

Using an AS16 column with 70/30 (v/v) acetonitrile/1 M aqueous methylamine as the mobile phase, the non-suppressed IC-ESI-MS/MS method can achieve sub-μg/L detection limits for chloro-, bromo- and iodoacetic acids, with 83.9–110.0% recoveries, 3.3–7.1% intra-day signal area RSDs and 3.4–10.4% inter-day signal area RSDs. This method was also applied and validated for monitoring HAA formation during chlorination experiments and for analyses of HAA levels in tap waters and a wastewater effluent.

CRediT authorship contribution statement

Shi Cheng: Investigation, Visualization and Writing. **Ya-Ping Wu:** Investigation. **Tessora R. Young:** Data curation and Discussion. **Michael C. Dodd:** Data curation, Discussion and Writing. **Ji Wu:** Investigation. **Hao Zhang:** Investigation. **Zong-Li Huo:** Investigation and Resources. **Yu-Ting Qian:** Investigation and Resources. **Yan Li:** Discussion. **Wen-Tao Li:** Conceptualization, Funding acquisition, Methodology, Investigation and Writing. **Ai-Min Li:** Conceptualization, Resources and Discussion.

Declaration of competing interest

The authors declare that they have no known competing financial interests or personal relationships that could have appeared to influence the work reported in this paper.

Acknowledgments

This study was financially supported by the National Natural Science Foundation of China (51708279), Basic Research Program of Jiangsu Province (BK20170642), and National Key Research and Development Program (2016YFE0112300). M.C.D and T.R.Y. acknowledge support provided by the U.S. National Science Foundation through Grant No. CBET-1236303. Additional support for T.R.Y. from a National Science Foundation Graduate Research Fellowship (ID: 2015177669) is gratefully acknowledged.

We also thank **Mr**. **Bolin Liu** from Anhui Province Center for Disease Control and Prevention, **Mrs**. **Wen Xiong** from Chengdu Institute for Food and Drug Control, **Mr**. **Shengbing Yu** from Guangdong Province Center for Disease Control and Prevention and **Mr**. **Kun Hou** from Inner Mongolia Autonomous Region Center for Disease Control and Prevention, for their contributions to the validation of this non-suppressed IC-ESI-MS/MS method as the national standard method for HAAs analysis in drinking water.

Appendix A. Supplementary data

Supplementary data to this article can be found online at https://doi.org/10.1016/j.scitotenv.2020.142297.

References

Barron, L., Paull, B., 2004. Determination of haloacetic acids in drinking water using suppressed micro-bore ion chromatography with solid phase extraction. Anal. Chim. Acta 522, 153–161. https://doi.org/10.1016/j.aca.2004.06.052.

Cardador, M.J., Serrano, A., Gallego, M., 2008. Simultaneous liquid–liquid microextraction/methylation for the determination of haloacetic acids in drinking waters by headspace gas chromatography. J. Chromatogr. A 1209, 61–69. https://doi.org/10.1016/j.chroma.2008.09.033.

Chen, C., Zhang, X.-j., Zhu, L.-x., Liu, J., He, W.-j., H-d, Han, 2008. Disinfection by-products and their precursors in a water treatment plant in North China: seasonal changes and fraction analysis. Sci. Total Environ. 397, 140–147. https://doi.org/10.1016/j.scitotenv.2008.02.032.

DeMarini, D.M., 2020. A review on the 40th anniversary of the first regulation of drinking water disinfection by-products. Environ. Mol. Mutagen. 61, 588–601. https://doi.org/10.1002/em.22378.

Dixon, A.M., Delinsky, D.C., Bruckner, J.V., Fisher, J.W., Bartlett, M.G., 2004. Analysis of dichloroacetic acid in drinking water by ion exchange HILIC-LC/MS/MS. J. Liq. Chromatogr. Relat. Technol. 27, 2343–2355.

Espinosa, S., Bosch, E., Rosés, M., 2002. Retention of ionizable compounds in high-performance liquid chromatography: 14. Acid–base pK values in acetonitrile–water mobile phases. J. Chromatogr. A 964, 55–66. https://doi.org/10.1016/S0021-9673(02)00558-7.

Gallidabino, M.D., Hamdan, L., Murphy, B., Barron, L.P., 2018. Suspect screening of halogenated carboxylic acids in drinking water using ion exchange chromatography – high resolution (Orbitrap) mass spectrometry (IC-HRMS). Talanta 178, 57–68. https://doi.org/10.1016/j.talanta.2017.08.092.

Gilchrist, E.S., Nesterenko, P.N., Smith, N.W., Barron, L.P., 2015. Organic solvent and temperature-enhanced ion chromatography-high resolution mass spectrometry for the determination of low molecular weight organic and inorganic anions. Anal. Chim. Acta 865, 83–91. https://doi.org/10.1016/j.aca.2015.01.031.

Hu, S., Gong, T., Ma, J., Tao, Y., Xian, Q., 2018. Simultaneous determination of iodinated haloacetic acids and aromatic iodinated disinfection byproducts in waters with a new SPE-HPLC-MS/MS method. Chemosphere 198, 147–153. https://doi.org/10.1016/j.chemosphere.2018.01.124.

Kinani, A., Kinani, S., Richard, B., Lorthioy, M., Bouchonnet, S., 2016. Formation and determination of organohalogen by-products in water - part I. Discussing the parameters influencing the formation of organohalogen by-products and the relevance of estimating their concentration using the AOX (adsorbable organic halide) method.

Trac-Trends in Analytical Chemistry 85, 273–280. https://doi.org/10.1016/j.trac.2016.06.008.
Kinani, A., Olivier, J., Roumiguieres, A., Bouchonnet, S., Kinani, S., 2018. A sensitive and specific solid-phase extraction-gas chromatography-tandem mass spectrometry method for the determination of 11 haloacetic acids in aqueous samples. European Journal of Mass Spectrometry 24, 375–383. https://doi.org/10.1177/1469066718781302.
Krasner, S.W., McGuire, M.J., Jacangelo, J.G., Patania, N.L., Reagan, K.M., Marco Aieta, E., 1989. Occurrence of disinfection by-products in US drinking water. Journal American Water Works Association 81, 41–53.
Krasner, S.W., Weinberg, H.S., Richardson, S.D., Pastor, S.J., Chinn, R., Sclimenti, M.J., et al., 2006. Occurrence of a new generation of disinfection byproducts. Environmental Science & Technology 40, 7175–7185. https://doi.org/10.1021/es060353j.
Kumar, K., Day, R.A., Margerum, D.W., 1986. Atom-transfer redox kinetics: general-acid-assisted oxidation of iodide by chloramines and hypochlorite. Inorg. Chem. 25, 4344–4350. https://doi.org/10.1021/ic00244a012.
Li, Y., Whitaker, J.S., McCarty, C.L., 2012. Analysis of iodinated haloacetic acids in drinking water by reversed-phase liquid chromatography/electrospray ionization/tandem mass spectrometry with large volume direct aqueous injection. J. Chromatogr. A 1245, 75–82. https://doi.org/10.1016/j.chroma.2012.05.005.
Liu, Y., Mou, S., 2003. Simultaneous determination of trace level bromate and chlorinated haloacetic acids in bottled drinking water by ion chromatography. Microchem. J. 75, 79–86. https://doi.org/10.1016/S0026-265X(03)00055-9.
Liu, Y., Mou, S., Chen, D., 2004. Determination of trace-level haloacetic acids in drinking water by ion chromatography–inductively coupled plasma mass spectrometry. J. Chromatogr. A 1039, 89–95. https://doi.org/10.1016/j.chroma.2003.12.069.
Luo, Q., Wang, D., Wei, Z., Wang, Z., 2013. Optimized chromatographic conditions for separation of halogenated acetic acids by ultra-performance liquid chromatography–electrospray ionization-mass spectrometry. J. Chromatogr. A 1277, 26–34. https://doi.org/10.1016/j.chroma.2012.12.046.
Meng, L., Wu, S., Ma, F., Jia, A., Hu, J., 2010. Trace determination of nine haloacetic acids in drinking water by liquid chromatography–electrospray tandem mass spectrometry. J. Chromatogr. A 1217, 4873–4876. https://doi.org/10.1016/j.chroma.2010.04.074.
USEPA, 2009. Method 557, Version 1.0. Determination of Haloacetic Acids, Bromate, and Dalapon in Drinking Water by Ion Chromatography Electrospray Ionization Tandem Mass Spectrometry. pp. 41320–45268.
Paull, B., Barron, L., 2004. Using ion chromatography to monitor haloacetic acids in drinking water: a review of current technologies. J. Chromatogr. A 1046, 1–9. https://doi.org/10.1016/j.chroma.2004.06.081.
Richardson, S.D., 2011. Disinfection by-products: formation and occurrence in drinking water. In: Nriagu, J.O. (Ed.), Encyclopedia of Environmental Health. Elsevier, Burlington, pp. 110–136.
Richardson, S.D., Plewa, M.J., Wagner, E.D., Schoeny, R., DeMarini, D.M., 2007. Occurrence, genotoxicity, and carcinogenicity of regulated and emerging disinfection by-products in drinking water: a review and roadmap for research. Mutation Research-Reviews in Mutation Research 636, 178–242. https://doi.org/10.1016/j.mrrev.2007.09.001.
Richardson, S.D., Fasano, F., Ellington, J.J., Crumley, F.G., Buettner, K.M., Evans, J.J., et al., 2008. Occurrence and mammalian cell toxicity of iodinated disinfection byproducts in drinking water. Environmental Science & Technology 42, 8330–8338. https://doi.org/10.1021/es801169k.
Roehl, R., Slingsby, R., Avdalovic, N., Jackson, P.E., 2002. Applications of ion chromatography with electrospray mass spectrometric detection to the determination of environmental contaminants in water. J. Chromatogr. A 956, 245–254. https://doi.org/10.1016/S0021-9673(02)00041-9.
Rossini, E., Bochevarov, A.D., Knapp, E.W., 2018. Empirical conversion of pKa values between different solvents and interpretation of the parameters: application to water, acetonitrile, dimethyl sulfoxide, and methanol. Acs Omega 3 (2), 1653–1662. https://doi.org/10.1021/acsomega.7b01895.
Sarrión, M.N., Santos, F.J., Galceran, M.T., 1999. Solid-phase microextraction coupled with gas chromatography–ion trap mass spectrometry for the analysis of haloacetic acids in water. J. Chromatogr. A 859, 159–171. https://doi.org/10.1016/S0021-9673(99)00873-0.
Shi, H., Adams, C., 2009. Rapid IC–ICP/MS method for simultaneous analysis of iodoacetic acids, bromoacetic acids, bromate, and other related halogenated compounds in water. Talanta 79, 523–527. https://doi.org/10.1016/j.talanta.2009.04.037.
Singer, P.C., Obolensky, A., Greiner, A., 1995. DBPs in chlorinated North Carolina drinking waters. Journal American Water Works Association 87, 83–92.
Teh, H.B., Li, S.F.Y., 2015. Simultaneous determination of bromate, chlorite and haloacetic acids by two-dimensional matrix elimination ion chromatography with coupled conventional and capillary columns. J. Chromatogr. A 1383, 112–120. https://doi.org/10.1016/j.chroma.2015.01.037.
Urbansky, E.T., 2000. Techniques and methods for the determination of haloacetic acids in potable water. J. Environ. Monit. 2, 285–291. https://doi.org/10.1039/B002977G.
USEPA, 2005a. Method 331.0, Determination of Perchlorate in Drinking Water by Liquid Chromatography Electrospray Ionization Mass Spectrometry.
USEPA, 2005b. Stage 1 and Stage 2 Disinfectants and Disinfection Byproducts Rules.
Wagner, E.D., Plewa, M.J., 2017. CHO cell cytotoxicity and genotoxicity analyses of disinfection by-products: an updated review. J. Environ. Sci. 58, 64–76. https://doi.org/10.1016/j.jes.2017.04.021.
Wang, J., Gong, T., Xian, Q., 2020. Formation of haloacetic acids from different organic precursors in swimming pool water during chlorination. Chemosphere 247, 125793. https://doi.org/10.1016/j.chemosphere.2019.125793.
Wu, S., Anumol, T., Gandhi, J., Snyder, S.A., 2017. Analysis of haloacetic acids, bromate, and dalapon in natural waters by ion chromatography–tandem mass spectrometry. J. Chromatogr. A 1487, 100–107. https://doi.org/10.1016/j.chroma.2017.01.006.
Xue, R., Donovan, A., Shi, H., Yang, J., Hua, B., Inniss, E., et al., 2016. Rapid simultaneous analysis of 17 haloacetic acids and related halogenated water contaminants by high-performance ion chromatography-tandem mass spectrometry. Anal. Bioanal. Chem. 408, 6613–6622. https://doi.org/10.1007/s00216-016-9773-8.
Xue, R., Shi, H., Ma, Y., Yang, J., Hua, B., Inniss, E.C., et al., 2017. Evaluation of thirteen haloacetic acids and ten trihalomethanes formation by peracetic acid and chlorine drinking water disinfection. Chemosphere 189, 349–356. https://doi.org/10.1016/j.chemosphere.2017.09.059.
Yang, M., Zhang, X., 2013. Comparative developmental toxicity of new aromatic halogenated DBPs in a chlorinated saline sewage effluent to the marine polychaete Platynereis dumerilii. Environmental Science & Technology 47, 10868–10876. https://doi.org/10.1021/es401841t.
Zhao, C., Fujii, Y., Yan, J., Harada, K.H., Koizumi, A., 2015. Pentafluorobenzyl esterification of haloacetic acids in tap water for simple and sensitive analysis by gas chromatography/mass spectrometry with negative chemical ionization. Chemosphere 119, 711–718. https://doi.org/10.1016/j.chemosphere.2014.07.048.
Zheng, L.L., Sun, H.J., Wu, C.Y., Wang, Y.B., Zhang, Y.Y., Ma, G.C., et al., 2020. Precursors for brominated haloacetic acids during chlorination and a new useful indicator for bromine substitution factor. Sci. Total Environ. 698. https://doi.org/10.1016/j.scitotenv.2019.134250.